metals

MDPI

Article

Study of the Morphological and Structural Features of Inert Matrices Based on ZrO_2–CeO_2 Doped with Y_2O_3 and the Effect of Grain Sizes on the Strength Properties of Ceramics

Artem L. Kozlovskiy [1,2,*], Maxim V. Zdorovets [1,2] and Dmitriy I. Shlimas [1,2]

[1] Laboratory of Solid State Physics, The Institute of Nuclear Physics, Almaty 050032, Kazakhstan
[2] Engineering Profile Laboratory, L.N. Gumilyov Eurasian National University, Nur-Sultan 010008, Kazakhstan
* Correspondence: kozlovskiy.a@inp.kz; Tel./Fax: +7-7024413368

Abstract: This article is devoted to the study of the mechanical and strength properties of Y_2O_3-doped ZrO_2–CeO_2 composite ceramics. The choice of these ceramics is due to their prospects in the field of nuclear energy, structural materials and as the basis for materials of dispersed nuclear fuel inert matrices. The choice as objects for research is due to their physicochemical, insulating and strength properties, the combination of which makes it possible to create one of the promising types of composite ceramics with high resistance to external influences, high mechanical pressures and crack resistance. The method of mechanochemical synthesis followed by thermal annealing of the samples at a temperature of 1500 °C; was used as a preparation method; to study the effect of Y_22O_3 doping, scanning electron microscopy methods were used to determine morphological features. The X-ray diffraction method was applied to determine the structural features and phase composition. The mechanical methods of microindentation and single compression for determination were applied to determine the strength characteristics. During the tests, it was found that the most resistant materials to external mechanical influences, and thermal heating for a long time of testing, are ceramics, in which the $CeZrO_4$ phase dominates. At the same time, the strengthening of ceramics and an increase in crack resistance is due to a change in the phase composition and to a decrease in the grain size, leading to the formation of a large dislocation density, and, consequently, the appearance of the dislocation strengthening effect. The relevance and novelty of this study lies in obtaining new types of ceramic materials for inert matrices of nuclear fuel, studying their morphological, structural, strength and thermophysical properties, as well as assessing their resistance to external influences during prolonged thermal heating. The results obtained can later be used as fundamental knowledge in assessing the prospects for the use of oxide ceramics as nuclear materials.

Keywords: composite ceramics; strength properties; zirconium dioxide; yttrium; doping; size factor; inert nuclear fuel

Citation: Kozlovskiy, A.L.; Zdorovets, M.V.; Shlimas, D.I. Study of the Morphological and Structural Features of Inert Matrices Based on ZrO_2–CeO_2 Doped with Y_2O_3 and the Effect of Grain Sizes on the Strength Properties of Ceramics. *Metals* **2022**, *12*, 1687. https://doi.org/10.3390/met12101687

Academic Editor: Florin Miculescu

Received: 16 August 2022
Accepted: 29 September 2022
Published: 10 October 2022

1. Introduction

In recent decades, great interest has been directed to solving issues related to the study of alternative methods for increasing the efficiency of using nuclear fuel, including increasing the degree of fuel burnup in fuel rods [1,2]. Another important issue in this direction is the study of the possibility of switching from nuclear fuel from uranium to non-uranium fuel, which can be based on plutonium [3,4]. The basis for these studies is the need to reduce the concentration of nuclear cycle waste, which includes the accumulation of plutonium as one of the decay products, and the processing of weapons-grade plutonium to use for peaceful purposes, as well as to reduce its stocks [5,6]. Unlike uranium fuel, the use of plutonium as a nuclear fuel will reduce the concentration of long-lived nuclear waste, as well as recycle existing stocks of weapons-grade plutonium. In addition, the use of plutonium as a basis for nuclear fuel requires new technological solutions in terms of increasing the productivity and efficiency of fuel burnup, the possibility of operating for

a long time at elevated temperatures, as well as in the field of mechanical impacts and resistance to external pressures or deformations [7–10].

To solve these conditions, one of the options for creating new types of nuclear fuel is the transition to fuel based on inert matrices [11,12]. This type of fuel is based on a technological solution, which consists in the fact that nuclear fuel is placed in dispersed ceramics, which serve as both an absorber and a heat transfer material [13,14]. At the same time, the key requirement for an inert matrix based on oxide or nitride refractory ceramics is their resistance to both radiation damage caused by irradiation and mechanical stress, cracking, external pressure, etc. This requirement is due to the fact that during operation these inert matrix materials will be subjected to both deformation processes caused by the accumulation of radiation damage and external influences associated with temperature changes, thermal expansion, mechanical pressures, etc. [15–17]. At the same time, the choice of oxide refractory ceramics as the basis for inert matrices is due to their properties, the combination of which allows us to assume that these materials are very promising in this direction.

Recently, great interest among oxide ceramics has been given to compounds of zirconium dioxide and cerium, which is due to their high strength, thermal conductivity and heat capacity. However, one of the key disadvantages of zirconium dioxide is its low resistance to polymorphic transformations, which can be initiated as a result of external influences, including irradiation [18,19]. To eliminate this disadvantage, as a rule, various stabilizing dopants are used, which inhibit the transformation processes and increase resistance to external influences.

Another promising direction in this area is to increase the resistance to mechanical damage due to size and dislocation effects. This conjecture is that small grain sizes and high dislocation density have a strengthening effect on the material due to the creation of additional obstacles to the propagation of cracks and deformation inclusions in the structure under mechanical loads [20–24].

The purpose of this study is to establish patterns of the effect of grain sizes on the strength and mechanical properties of composite ceramics to cracking processes, as well as to determine the dependence of the effect of the phase composition of ceramics on grain sizes and the dynamics of their change. Composite ceramics based on ZrO_2–CeO_2 compounds doped with Y_2O_3 obtained by solid-phase mechanochemical synthesis were selected as objects of study. The choice of research objects is due to their prospects for using inert matrix materials for dispersed nuclear fuel, the main purpose of which is to replace traditional nuclear fuel with uranium-free nuclear fuel, which has great prospects in the new generation of nuclear power [19–24]. As shown in a number of works, the formation of ceramics with the structure of complex oxides of the $Ce_{0.5}Zr_{0.5}O_2$ or $CeZrO_4$ type leads to an increase in the resistance of ceramics to external influences, as well as an increase in their productivity when used as a basis for catalysts, due to a change in the specific surface area and phase inclusions [25,26].

2. Experimental Part

To obtain the studied ZrO_2–CeO_2 samples doped with Y_2O_3, the method of solid-phase mechanochemical synthesis was chosen and implemented using standard technology. The micron powders of ZrO_2, CeO_2 and Y_2O_3 (Sigma Aldrich, Burlington, MA, USA) chemical compounds in specified stoichiometric ratios were used as initial components. The chemical purity of the compounds used for the synthesis was 99.95%. The Y_2O_3 dopant concentration varied from 5 to 15%.

Ceramics were synthesized by mechanochemical grinding using a PULVERISETTE 6 classic line planetary mill (Fritsch, Berlin, Germany). A glass made of tungsten carbide was used for mixing; the ratio of grinding balls (diameter 8 mm) and initial mixtures was 2:1. The grinding of the samples was carried out at a grinding speed of 400 rpm for 60 min. The choice of grinding speed, as well as grinding time, was carried out experimentally to obtain a homogeneous mixture after grinding, as well as to initiate phase transformation

processes as a result of deformation distortions in the grinding process. After grinding, the obtained mixtures were checked for the presence of impurity inclusions by the method of energy dispersive analysis. According to the obtained data, no impurities were found in the composition of the studied mixtures.

After grinding, the resulting mixtures were annealed in a muffle furnace at a temperature of 1500 °C for 5 h, the heating rate was 10 °C/min. After annealing, the samples were cooled for 24 h together with the furnace in order to avoid the effects of rapid oxidation in air. A Rus-Universal muffle furnace was used for annealing.

The morphological features of the synthesized samples and grain sizes were determined using the method of scanning electron microscopy, which was implemented on a Hitachi TM3030 (Hitachi, Japan) microscope. Image analysis for grain size determination and counting was performed using ImageJ image processing software.

The analysis of the structural characteristics and phase composition of the studied ceramics depending on the dopant concentration was carried out based on X-ray diffraction data obtained using a D8 Advance Eco X-ray diffractometer (Bruker, Germany). The diffraction patterns were obtained in the Bragg–Brentano geometry, in the angular range of 2θ = 25–90°. The DiffracEVA v.4.2 software was used to analyze the crystal lattice parameters.

The strength properties were measured by indentation and single compression of ceramic samples. During microhardness determination, a Vickers pyramid was used as an indenter. The single compression method consisted in compressing ceramic samples in a press at a constant compression rate of 0.1 mm/min until the pressure value was fixed at which microcracks were observed. Before testing, the samples were pressed into tablets 5 mm in diameter and 2 mm thick for compression experiments. The determination of resistance to cracking was evaluated by a comparative analysis of the obtained values of the maximum pressure at which the stage of cracking and fracture of ceramics occurs for different types of ceramics under study.

3. Results and Discussion

One of the methods for characterizing the properties of ceramics is the assessment of morphological changes depending on the phase composition, as well as the dopant concentration. Figure 1 shows the results of studies of changes in the grain morphology of the synthesized ZrO_2–CeO_2 composite ceramics. The general view of the observed changes in grain morphology depending on the concentration of the Y_2O_3 dopant indicates that the addition of Y_2O_3 during synthesis leads to a change in the grain size, shape and geometry, which may be due to phase transformation processes [27,28].

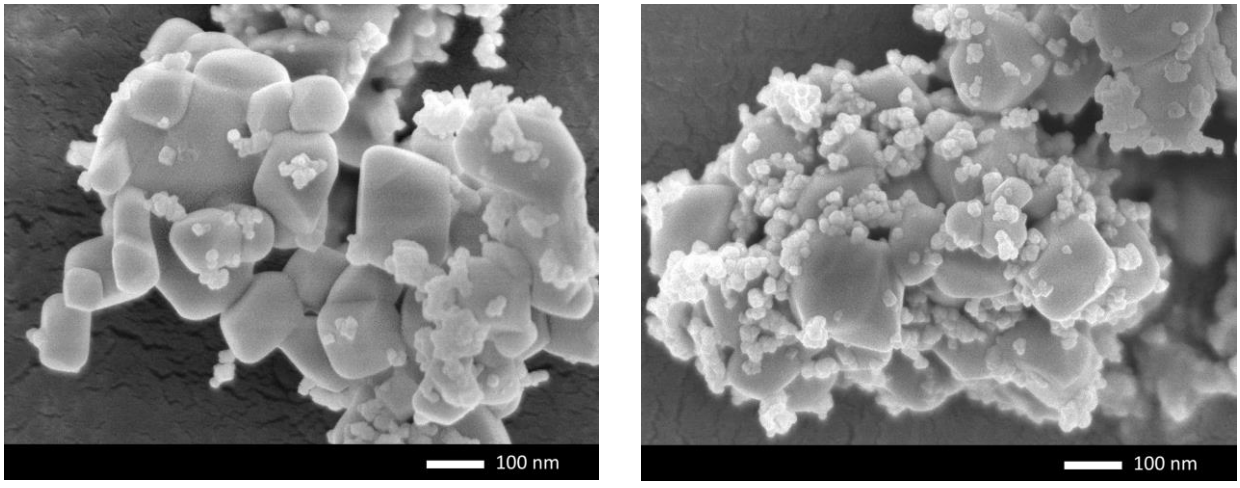

(**a**) (**b**)

Figure 1. *Cont.*

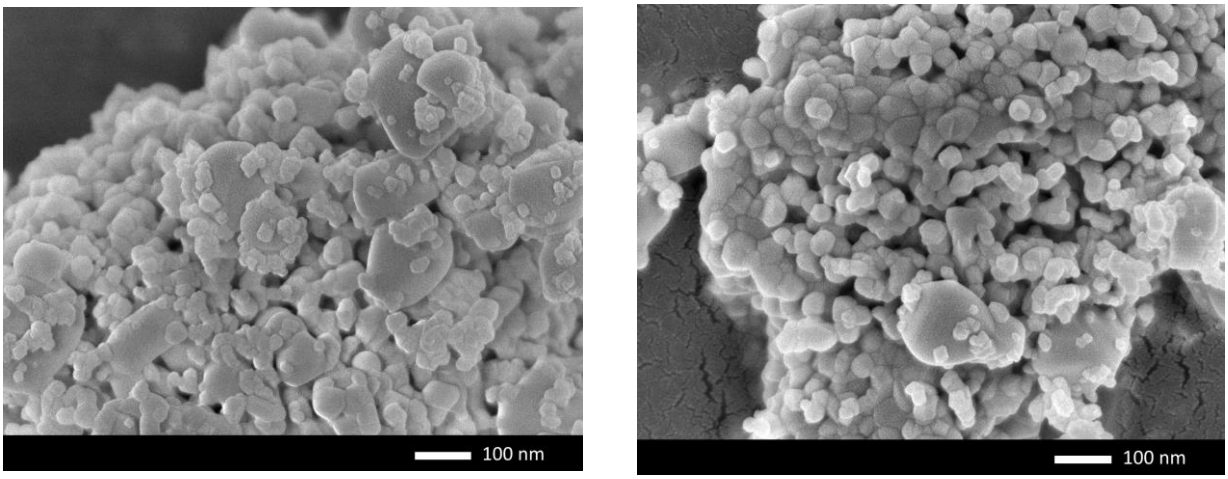

(**c**) (**d**)

Figure 1. Results of morphological studies of synthesized ZrO_2–CeO_2 ceramics depending on the Y_2O_3 dopant concentration: (**a**) Pristine sample; (**b**) 5%; (**c**) 10%; (**d**) 15%.

In the case of the original samples, the dominant type of grains are rhomboid grains, the size of which varies within 90–120 nm, which are surrounded by growths in the form of accumulations of small grains, dendritic or feather-shaped. The presence of two types of grains indicates that during the sintering of the initial mixtures, phase transformations occur, which are accompanied by the formation of grains of different geometries. Doping with Y_2O_3, as well as a further increase in its concentration, leads to the displacement of large rhomboid grains by smaller, spherical grains, which, at dopant concentrations of 10–15%, form a densely packed structure with a dendrite-like shape. A decrease in grain size, as well as their compaction, leads to an increase in boundary effects, as well as an increase in the specific surface area.

After analyzing the obtained SEM images of the synthesized ceramics in order to determine the grain sizes, as well as their homogeneity, grain size distribution diagrams were constructed. For the construction, the ImageJ program code was used, with the help of which the grain sizes were determined, as well as their geometry. The evaluation results are presented in Figure 2.

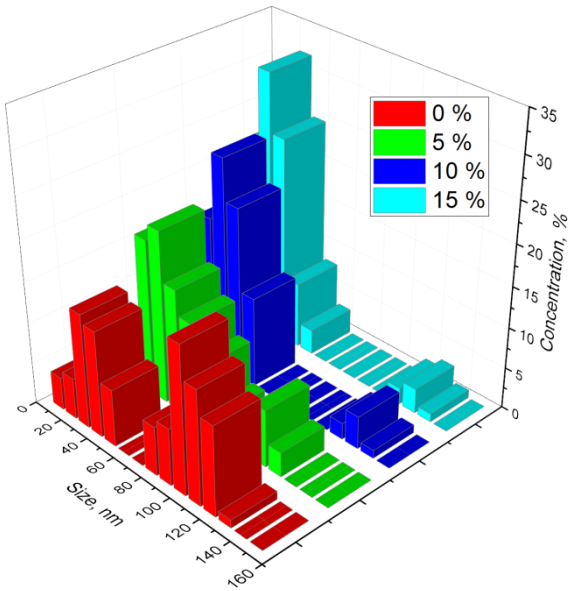

Figure 2. Size diagram obtained by analyzing grain sizes according to SEM image data.

As can be observed from the presented size diagrams in the case of the initial ceramics, there are two characteristic particle size distributions, which are typical for large grains, the sizes of which vary from 90 to 120 nm, and small spherical grains with sizes of 25–40 nm. At the same time, the ratio of the content of large and small grains is approximately 70/30 with the dominance of large grains. Doping with Y_2O_3 at a content of 5% leads to a decrease in the contribution of large grains in the composition of ceramics, as evidenced by the results of both size diagrams and SEM image data. In this case, a slight decrease in the average grain size is also observed, which indicates the recrystallization processes because of the addition of Y_2O_3, as well as the initialization of phase transformation processes.

At a Y_2O_3 dopant concentration of 10–15%, a decrease in the contribution of large grains is observed, which is no more than 3–5% of the total number of grains, and the diagram characteristic of small grain sizes becomes narrower in the size range, which indicates an increase in the grain size homogeneity degree. At the same time, the analysis of the obtained SEM images, as well as dimensional diagrams constructed on their basis, showed that in the case of Y_2O_3 dopant concentrations equal to 10–15%, the formation of a close-packed grain structure, similar in shape to dendrite-like types of structures, is observed. The formation of such types of structural and morphological features can be due to the processes of phase transformations that occur during thermal annealing of the samples. Further, the addition of Y_2O_3 can lead to the initialization of phase transformation processes, accompanied by recrystallization processes and a change in grain size.

In turn, an increase in the homogeneity degree in combination with a decrease in the grain size, as well as the formation of a close-packed structure, can have a significant effect on the strength characteristics of ceramics, as well as their resistance to external influences.

Figure 3a shows the results of X-ray phase analysis of the synthesized ceramics depending on the Y_2O_3 dopant concentration in the composition.

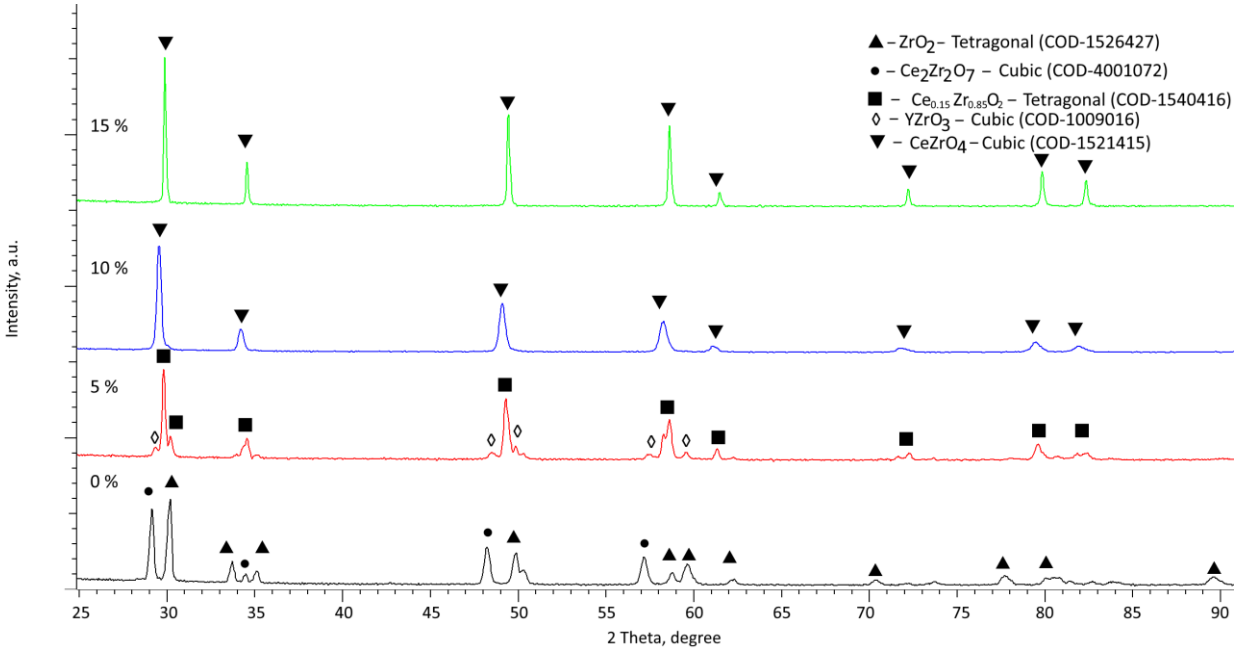

(**a**)

Figure 3. *Cont.*

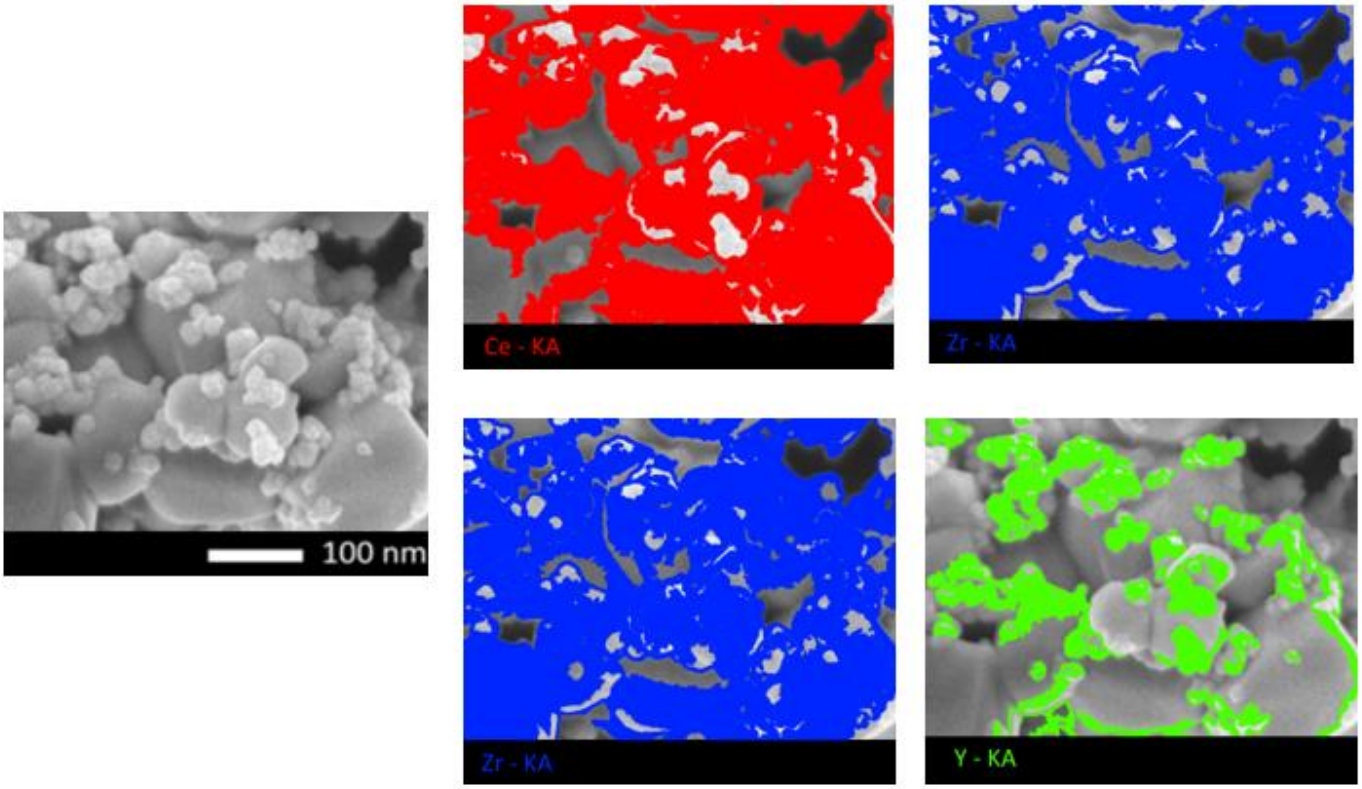

(**b**)

Figure 3. (**a**) Results of X-ray diffraction of the studied ceramics depending on the concentration of the Y_2O_3 dopant. (**b**) The results of mapping a ceramic sample with a dopant concentration of 5%.

The general form of the observed changes in the diffraction patterns indicates two processes occurring as a result of thermal sintering depending on the Y_2O_3 dopant concentration. The first type is associated with the appearance of new diffraction reflections with an increase in the Y_2O_3 dopant concentration, which indicates the processes of phase transformations and a change in the phase composition of the synthesized ceramics. These processes are most pronounced when the dopant concentration changes from 5 to 10%.

The second type of observed changes is typical for processes associated with structural ordering, which is expressed in a change in the shape of diffraction reflections, as well as their shift to the region of small angles, which indicates a decrease in the contributions of amorphous-like inclusions or disordered regions. At the same time, this type of changes is most pronounced for ceramic samples with an increase in the concentration of the Y_2O_3 dopant from 10 to 15%. In this case, the main changes observed in the diffraction pattern are characteristic only for the second type of changes, which are characterized by an increase in the symmetry of the shape of diffraction lines relative to the position of the maximum, as well as a decrease in the ratio of the areas of diffraction reflections and background radiation, which characterizes the structural ordering degree.

Analyzing the positions of diffraction maxima and their intensity by comparing with card values from the database, the phase composition of the studied samples was established. For initial samples without dopant, the phase composition of ceramics is a solid solution of two phases of tetragonal ZrO_2 (P42/nmc(137)) and cubic $Ce_2Zr_2O_7$ (Fm-3m(227)) in the ratio $ZrO_2/Ce_2Zr_2O_7$~87/23. The formation of such a structure is typical for ceramics obtained by mechanochemical synthesis followed by thermal annealing, as a result of which the processes of the partial substitution of ions of one type for ions of another type are initiated, followed by the formation of structures similar to a complex oxide.

In the case of the addition of the Y_2O_3 dopant to the mixture composition, according to the obtained X-ray diffraction data, we observed the appearance of new diffraction

reflections characteristic of the tetragonal $Ce_{0.15}Zr_{0.85}O_2$ phase, the formation of which is associated with the transformation of the ZrO_2 phase associated with the partial replacement of zirconium ions by cerium ions, as well as reflections characteristic of the $YZrO_3$ cubic phase, the content of which does not exceed 20%.

Figure 3b shows the results of mapping a sample with the Y_2O_3 dopant concentration of 5%, for which, according to SEM images, the presence of small spherical grains was established. As can be observed from the mapping data, these grains contain a sufficient amount of Zr and Y, and therefore, it can be concluded that these grains correspond to the cubic phase of $YZrO_3$.

When the Y_2O_3 dopant is added in the amount of 10–15%, the obtained data of X-ray diffraction patterns indicate the process of phase transformations of the $Ce_{0.15}Zr_{0.85}O_2$–Tetragonal/$YZrO_3$–Cubic → $CeZrO_4$–Cubic type with subsequent structural ordering of the cubic $CeZrO_4$ phase. This transformation is due to the fact that the addition of Y_2O_3, the melting point of which is much lower than the melting point of ZrO_2 and CeO_2, leads to the fact that the processes of phase transformations proceed more intensively with the formation of a structure of complex oxides, followed by its ordering, as evidenced by the results of estimating the crystal lattice parameters, presented in Table 1.

Table 1. Lattice parameter data.

Phase	Lattice Parameter, Å			
	Concentration of Y_2O_3,%			
	0	**5**	**10**	**15**
ZrO_2–tetragonal	a = 3.5971 ± 0.0024, c = 3.2233 ± 0.0016, V = 67.59 ± 1.12 Å^3	-	-	-
$Ce_2Zr_2O_7$–Cubic	a = 10.6443 ± 0.0034, V = 1206.00 ± 1.21 Å^3	-	-	-
$Ce_{0.15}Zr_{0.85}O_2$–Tetragonal	-	a = 3.6418 ± 0.0031, c = 5.2329 ± 0.0017, V = 69.40 ± 1.15 Å^3	-	-
$YZrO_3$–Cubic	-	a = 10.5307, V = 1167.84 ± 0.93 Å^3	-	-
$CeZrO_4$–Cubic	-	-	a = 10.47127 ± 0.0016, V = 1148.15 ± 1.16 Å^3	a = 10.3953 ± 0.0025, V = 1123.34 ± 0.96 Å^3

In a detailed analysis of the obtained diffraction patterns for samples with the Y_2O_3 dopant concentration of 10–15%, it was found that there were no impurity inclusions of the $YZrO_3$ phase, which was determined for samples with a dopant concentration of 5%. When analyzing the position of diffraction reflections for samples with 10% and 15% dopant concentrations, it was found that the dominant phase most fully describing the position of all observed reflections is the cubic phase of $CeZrO_4$. However, using the Rietveld method, it was also found that when approximating these lines by the necessary functions, one can make an assumption that these reflections also correspond to the characteristic phase of $YZrO_3$, however, due to the close position of the lines of the two phases $YZrO_3$ and $CeZrO_4$ and the similarity of the crystal lattice parameters, it can be determined with a high degree of certainty that the contribution of the $YZrO_3$ phase for samples with a dopant concentration of 10–15% failed. In connection with this, an assumption was made about the complete dominance of the $CeZrO_4$ phase in the composition of ceramics at these concentrations, with the possible presence of inclusions of the $YZrO_3$ phase in the form of a solid solution.

As can be observed from the data presented in Table 1, the formation of the $CeZrO_4$ phase at a dopant concentration of 10% with a subsequent increase in concentration leads

to structural ordering of the crystal lattice, which is expressed in a decrease in the lattice parameters and volume.

According to the assessment results of the phase composition of the studied ceramics, depending on the dopant concentration, phase transformations can be written in the following form: ZrO_2–Tetragonal/$Ce_2Zr_2O_7$ –Cubic → $Ce_{0.15}Zr_{0.85}O_2$–Tetragonal/$YZrO_3$–Cubic → $CeZrO_4$–Cubic.

As is known, the formation of multiphase structures or structures of the type of a complex oxide or substitution can have a significant impact on the strength characteristics, as well as the resistance of ceramics to external influences, including thermal heating or exposure to aggressive media. The hardening effects in this case can be explained as the presence of interfacial boundaries or size effects associated with small grain sizes, which create additional obstacles to crack propagation and create barriers to their growth.

Figure 4 shows the results of measuring the strength characteristics of the studied ceramics, reflecting the effect of the dopant, as well as grain sizes and phase composition on hardening and increasing resistance to mechanical stress.

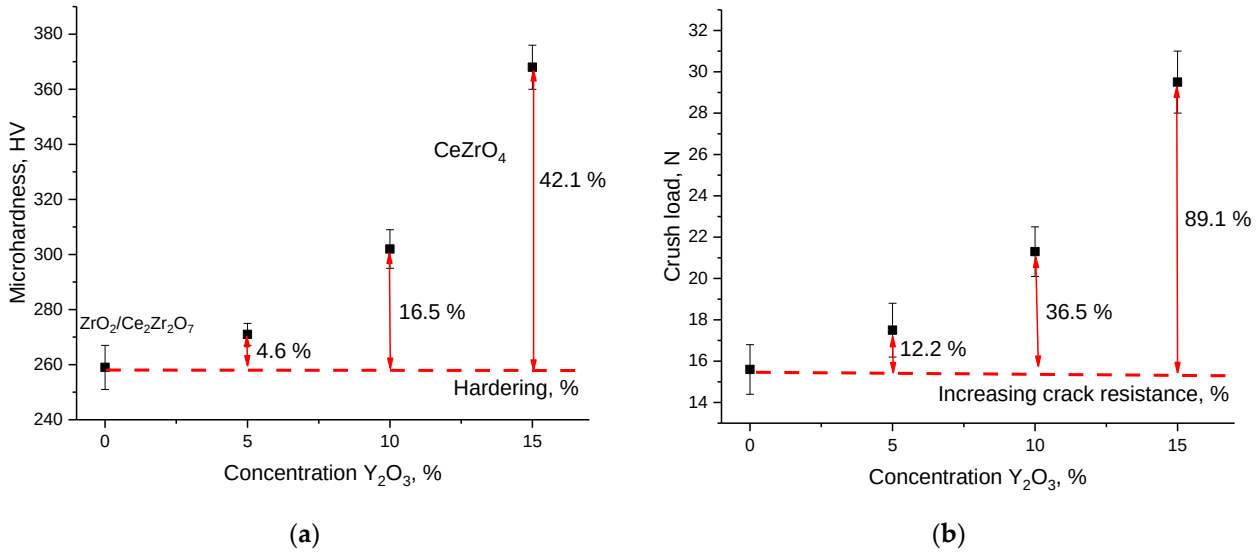

Figure 4. (**a**) Results of the microhardness value change depending on the dopant concentration. (**b**) Results of changes in the single compression resistance of ceramics depending on the dopant concentration.

An analysis of the changes in the microhardness obtained using the indentation method showed that with an increase in the dopant concentration, the surface of the ceramics is strengthened, as well as a decrease in the degree of softening, which is expressed in a decrease in the indenter print. At the same time, the most pronounced changes are observed for samples in which the $CeZrO_4$ phase dominates, for which the hardening in comparison with the original sample increased by 16.5% and 42.1%, respectively. It should be noted that the increase in hardening from 16.5% to 42.1% for single-phase samples is also due to the effect of structural ordering, which is observed in the analysis of structural parameters and the structural ordering degree obtained by interpreting X-ray diffraction data. Additionally, the hardness increase effect is due to the size effect associated with a change in grain size and morphology, as well as an increase in the size homogeneity degree (see data in Figure 2). A decrease in grain size leads to the formation of a close-packed structure consisting of small grains with many grain boundaries. Such a formation leads to the appearance of a strengthening effect associated with the creation of resistance to external influences due to the boundary and dislocation effects.

These effects are most pronounced when analyzing the results for determining the crack resistance under single compression of the samples, which are presented in Figure 4b.

An analysis of the data on crack resistance showed that the change in these values has a pronounced dependence not only on the phase composition of ceramics, but also on size effects that cause a change in dislocation density.

Figure 5 shows the results of a comparison of the effect of a change in the dislocation density on the strengthening of ceramics depending on the concentration of the Y_2O_3 dopant. As is known, the dislocation density (δ) has an inverse quadratic dependence on the grain size (D), which is expressed using the following expression $\delta = 1/D^2$. According to this expression, it can be concluded that with a decrease in the grain size, the dislocation density increases, which, as shown in a number of works [29–32], can lead to a strengthening effect and also explain the increase in the strength characteristics of ceramics. The effect of hardening with a change in the dislocation density is associated with an increase in intergranular and interfacial boundaries, the presence of which leads to an increase in the resistance to the propagation of microcracks in depth. At the same time, as can be observed from the presented dislocation density estimation data, an order of magnitude (~10^{10} cm^{-2}) is typical for structures with a large number of dislocations, as well as fine-grained structures, which can have a significant effect on the strengthening effect and increase resistance to destruction under external influences. According to the obtained data, an increase in the dislocation density with increasing dopant concentration is associated with a decrease in size and the formation of a denser packing of grains, which is clearly observed in the presented SEM images (see Figure 1).

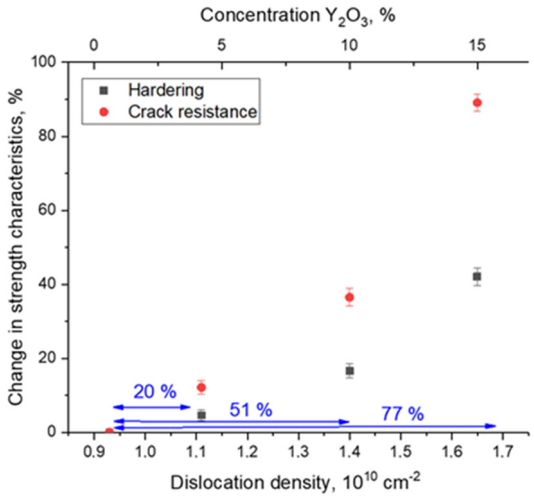

Figure 5. Comparison results of dislocation density changes on ceramic hardening.

The data presented in the figure for comparing changes in the dislocation density and hardening values indicate a positive effect of the influence of an increase in the dislocation density on the resistance of ceramics to external influences and mechanical pressure. As can be observed from the data presented, changes in the dislocation density by 20% do not lead to significant changes in the hardening of ceramics, while an increase in the dislocation density by more than 50% leads to significant changes in the strength characteristics. At the same time, it should be noted that the change in dislocation density has the greatest influence on the increase in resistance to cracking in a single compression. In this case, this effect can be explained by the fact that the formation of additional dislocations in the structure with a decrease in the grain size leads to a decrease in the propagation rate of microcracks in the structure under compression or other mechanical action, due to the appearance of additional obstacles in the form of grain boundaries or interfacial boundaries, containing many dislocations in their vicinity. A similar effect was observed in several works [29–32], in which the authors attribute the effect of dislocation hardening to a change in grain size and density.

As is known, the formation of substitutional structures or complex oxides of the $CeZrO_4$ type can lead not only to the strengthening of the mechanical properties of ceramics,

but also to an increase in the thermal stability of ceramics. An increase in resistance to long-term operation at elevated temperatures is one of the important criteria for using ceramics as inert matrix materials for nuclear fuel. During high-temperature operation, structural degradation processes associated with oxidative processes can be initiated, leading to destruction and a decrease in strength properties. To assess the influence of the phase composition, as well as the size effects associated with the grain size on the resistance to long-term thermal action, several experiments were carried out to test the resistance of the synthesized ceramics to thermal heating. The tests were carried out in an air atmosphere and the samples were subjected to thermal heating at a temperature of 700 °C for 200 h. Every 50 h, some of the samples were taken to determine the strength characteristics. The choice of annealing temperature for testing is due to the possibility of modeling the effects of temperature effects comparable to the heating temperature of nuclear fuel located in the reactor core. The results of the experiments are shown in Figure 6.

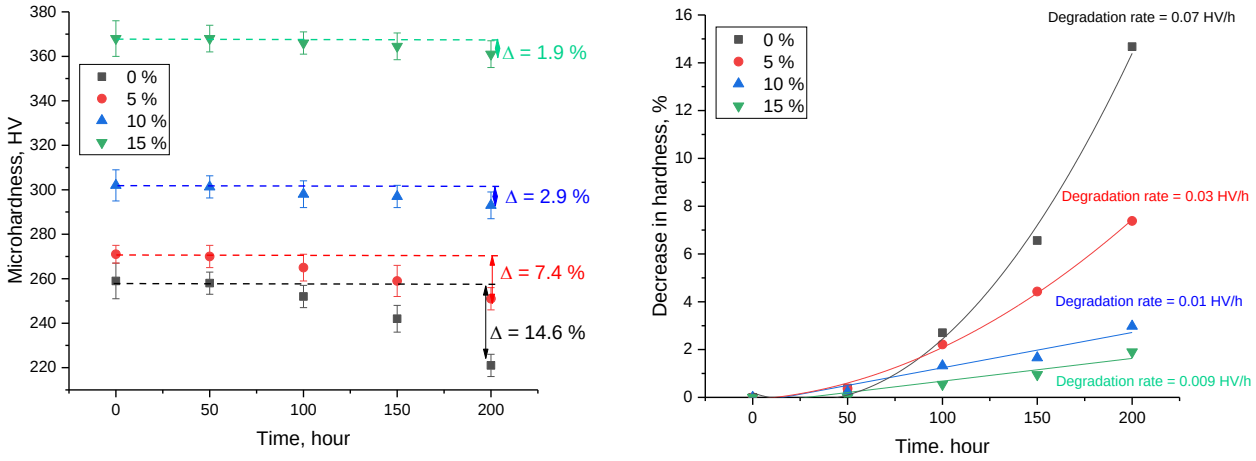

(**a**) (**b**)

Figure 6. The results of high-temperature tests for resistance to external influences: (**a**) Change in microhardness depending on the test time (the dotted lines indicate the microhardness of ceramics in the initial state, which are given as a comparison to assess the trend of changes); (**b**) Data of change in the degradation and hardness decrease rate.

The presented results of changes in hardness during high-temperature heating reflect the resistance of ceramics to degradation processes and reflect changes in the thermal stability of the samples. As can be observed from the data presented, the main changes associated with a decrease in hardness for the original samples are observed after 50 h of annealing, while for doped samples with a Y_2O_3 dopant concentration of 10–15%, changes are observed only after 100 h of testing. At the same time, the difference in hardness values for samples with a concentration of 10–15% is less than 3%, which indicates a high thermal stability of the samples. This thermal stability may be due to the fact that the formed cubic phase of $CeZrO_4$ has an increased resistance to thermal action and oxidation processes, which can be accompanied by partial disordering when oxygen is introduced from the atmosphere into interstices [33]. In addition, an increase in softening resistance for doped ceramics can be explained by the effect of dislocation hardening and the presence of a large number of grain boundaries, the presence of which leads to hardening and a decrease in the degradation rate. An estimate of the hardness and softening decrease rate, presented in Figure 6b, indicates that the formation of the $CeZrO_4$ phase in the structure of ceramics and its subsequent ordering with the dopant concentration increase leads to a decrease in the hardness degradation rate by almost an order of magnitude, and the change in hardness after 200 h of thermal testing does not exceeds 2–3%, which indicates a high resistance of the material to softening as a result of prolonged heating. Analyzing the obtained data, we can conclude that the formation of the $CeZrO_4$ phase in the structure of ceramics leads

to the creation of additional boundary interfacial effects that prevent the propagation of microcracks as a result of aging and also significantly increase the resistance of ceramics to mechanical stress under compression or external pressure.

The results of the experiments carried out are in good agreement with similar types of ceramics—candidate materials for nuclear fuel based on oxide or binary compounds. In particular, the results of resistance to long-term thermal heating of samples with a dopant concentration of 10–15% indicate a fairly high resistance to high-temperature degradation, which can serve as one of the key factors in considering these materials as alternative materials for inert matrices based on MgO, $MgAl_2O_4$ and other types of oxide ceramics [34–38].

4. Conclusions

The paper presents the assessment results of the resistance of ZrO_2–CeO_2-based ceramics doped with Y_2O_3 to mechanical stress under single compression, friction and external pressure. During the studies carried out, the main emphasis was placed on the study of the influence of the size factor due to the change in grain sizes depending on the phase composition of composite ceramics, as well as the influence of the yttrium dopant concentration on the increase in the resistance of composite ceramics to mechanical damage.

An analysis of the morphological features of the synthesized ceramics showed that an increase in the concentration of the dopant in the composition of the ceramics leads to a decrease in the grain size, as well as an increase in the degree of grain size homogeneity. At the same time, in the case of Y_2O_3 dopant concentrations of 10–15%, the formation of a close-packed structure is observed, accompanied by an increase in boundary effects.

During the phase analysis, it was found that with an increase in the concentration of the Y_2O_3 dopant to 10–15%, phase transformations of the $Ce_{0.15}Zr_{0.85}O_2$–Tetragonal/$YZrO_3$–Cubic → $CeZrO_4$–Cubic type occur in the ceramic structure, followed by the dominance of the $CeZrO_4$ phase and its structural ordering.

An assessment of the strength characteristics of the studied ceramics depending on the dopant concentration showed that a change in the phase composition, as well as a decrease in grain size, leads to strengthening and an increase in the resistance of ceramics to mechanical stress.

The results of thermal tests showed that the formation of the $CeZrO_4$ phase in the ceramic structure and a decrease in the grain size lead to an increase in the degradation resistance and the preservation of thermal stability during high-temperature heating.

Based on the studies conducted, it can be concluded that the doping of ceramics based on ZrO_2–CeO_2 compounds with Y_2O_3 dopant at a concentration of 10–15% leads to the formation of nanostructured single-phase ceramics with the cubic $CeZrO_4$ phase, which have a high degree of resistance to both mechanical stress and thermal heating. The resulting ceramics will be tested for radiation resistance to heavy ion irradiation and subsequent radiation embrittlement depending on the radiation dose.

Author Contributions: Conceptualization, D.I.S. and A.L.K.; methodology, M.V.Z. and A.L.K.; formal analysis, M.V.Z., D.I.S. and A.L.K.; investigation, M.V.Z., D.I.S. and A.L.K.; resources, A.L.K.; writing—original draft preparation, review and editing, D.I.S. and A.L.K.; visualization, A.L.K.; supervision, A.L.K. All authors have read and agreed to the published version of the manuscript.

Funding: This research was funded by the Science Committee of the Ministry of Education and Science of the Republic of Kazakhstan (No. BR11765580).

Institutional Review Board Statement: Not applicable.

Informed Consent Statement: Not applicable.

Data Availability Statement: Not applicable.

Acknowledgments: Not applicable.

Conflicts of Interest: The authors declare that they have no conflict of interest.

References

1. Ikonen, T.; Tulkki, V. The importance of input interactions in the uncertainty and sensitivity analysis of nuclear fuel behavior. *Nucl. Eng. Des.* **2014**, *275*, 229–241. [CrossRef]
2. MacDonald, P.E.; Lee, C.B. Use of thoria-urania fuels in PWRs: A general review of a NERI project to assess feasible core designs, economics, fabrication methods, in-pile thermal/mechanical behavior, and waste form characteristics. *Nucl. Technol.* **2004**, *147*, 1–7. [CrossRef]
3. Humphrey, U.E.; Khandaker, M.U. Viability of thorium-based nuclear fuel cycle for the next generation nuclear reactor: Issues and prospects. *Renew. Sustain. Energy Rev.* **2018**, *97*, 259–275. [CrossRef]
4. Lovecký, M.; Závorka, J.; Jiřičková, J.; Škoda, R. Increasing efficiency of nuclear fuel using burnable absorbers. *Prog. Nucl. Energy* **2020**, *118*, 103077. [CrossRef]
5. Keiser, D.D., Jr. Fuel cladding chemical interaction in metallic sodium fast reactor fuels: A historical perspective. *J. Nucl. Mater.* **2019**, *514*, 393–398. [CrossRef]
6. Lee, W.E.; Gilbert, M.; Murphy, S.T.; Grimes, R.W. Opportunities for advanced ceramics and composites in the nuclear sector. *J. Am. Ceram. Soc.* **2013**, *96*, 2005–2030. [CrossRef]
7. Parker, H.M.O.; Joyce, M.J. The use of ionising radiation to image nuclear fuel: A review. *Prog. Nucl. Energy* **2015**, *85*, 297–318. [CrossRef]
8. Galashev, A.Y. Recovery of actinides and fission products from spent nuclear fuel via electrolytic reduction: Thematic overview. *Int. J. Energy Res.* **2022**, *46*, 3891–3905. [CrossRef]
9. Galahom, A.A.; Sharaf, I.M. Finding a suitable fuel type for the disposal of the accumulated minor actinides in the spent nuclear fuel in PWR. *Prog. Nucl. Energy* **2021**, *136*, 103749. [CrossRef]
10. Kurniawan, T.A.; Othman, M.H.D.; Singh, D.; Avtar, R.; Hwang, G.H.; Setiadi, T.; Lo, W.-H. Technological solutions for long-term storage of partially used nuclear waste: A critical review. *Ann. Nucl. Energy* **2022**, *166*, 108736. [CrossRef]
11. Frieß, F.; Liebert, W. Inert-matrix fuel for transmutation: Selected mid-and long-term effects on reprocessing, fuel fabrication and inventory sent to final disposal. *Prog. Nucl. Energy* **2022**, *145*, 104106. [CrossRef]
12. Zhang, J.; Wang, H.; Wei, H.; Tang, C.; Lu, C.; Huang, C.; Ding, S.; Li, Y. Modelling of effective irradiation swelling for inert matrix fuels. *Nucl. Eng. Technol.* **2021**, *53*, 2616–2628. [CrossRef]
13. Wang, Y.; Wang, J.; Wang, J.; Li, X.; Tang, Y.; Li, N. Preparation of MgO-$Nd_2Zr_2O_7$ composite ceramics used for inert matrix fuel by one-step sintering method. *Ceram. Int.* **2022**, *48*, 27213–27216. [CrossRef]
14. Nandi, C.; Danny, K.; Bhattacharya, S.; Prakash, A.; Behere, P. Phase evolution in $M_{1-x}Pu_xO_2$ ($0.0 \leq x \leq 0.6$)(M = Zr, Th) as potential inert matrix fuel system under reducing and oxidizing conditions. *J. Nucl. Mater.* **2021**, *547*, 152800. [CrossRef]
15. Hudák, I.; Skryja, P.; Bojanovský, J.; Jegla, Z.; Krňávek, M. The Effect of Inert Fuel Compounds on Flame Characteristics. *Energies* **2021**, *15*, 262. [CrossRef]
16. Berguzinov, A.; Kozlovskiy, A.; Khametova, A.A.; Shlimas, D.I. Synthesis, Phase Transformations and Strength Properties of Nanostructured $(1-x)\ ZrO_2 - xCeO_2$ Composite Ceramics. *Nanomaterials* **2022**, *12*, 1979. [CrossRef] [PubMed]
17. Giniyatova, S.G.; Sailaukhanov, N.A.; Nesterov, E.; Zdorovets, M.V.; Kozlovskiy, A.L.; Shlimas, D.I. Research of Structural, Strength and Thermal Properties of ZrO_2—CeO_2 Ceramics Doped with Yttrium. *Crystals* **2022**, *12*, 242. [CrossRef]
18. Alin, M.; Kozlovskiy, A.L.; Zdorovets, M.V.; Uglov, V.V. Study of the mechanisms of the t-$ZrO_2 \rightarrow$ c-ZrO_2 type polymorphic transformations in ceramics as a result of irradiation with heavy Xe^{22+} ions. *Solid State Sci.* **2022**, *123*, 106791. [CrossRef]
19. Togatorop, E.; Suzuki-Muresan, T.; Harto, A.W. A review on the solubility of crystalline zirconium dioxide and thorium dioxide. *AIP Conf. Proc.* **2022**, *2501*, 030002.
20. Ivanov, I.A.; Rspayev, R.M.; Sapar, A.D.; Mustafin, D.A.; Zdorovets, M.V.; Kozlovskiy, A.L. Study of the Effect of Y_2O_3 Doping on the Resistance to Radiation Damage of CeO_2 Microparticles under Irradiation with Heavy Xe^{22+} Ions. *Crystals* **2021**, *11*, 1459. [CrossRef]
21. Jin, E.; Yuan, L.; Yu, J.; Ding, D.; Xiao, G. Enhancement of thermal shock and slag corrosion resistance of MgO–ZrO_2 ceramics by doping CeO_2. *Ceram. Int.* **2022**, *48*, 13987–13995. [CrossRef]
22. Zhao, L.; Jiang, Z.; Zhang, C.; Guo, W.; Jiang, Z.; Gao, X.; Cui, Y.; Shi, X. Theoretical modeling based on stress wave propagation and experimental verification of residual stress in stereolithography printed ZrO_2 ceramic suspensions. *Ceram. Int.* **2021**, *47*, 26935–26941. [CrossRef]
23. Fang, H.; Wang, W.; Huang, J.; Li, Y.; Ye, D. Corrosion behavior and thermos-physical properties of a promising Yb_2O_3 and Y_2O_3 co-stabilized ZrO_2 ceramic for thermal barrier coatings subject to calcium-magnesium-aluminum-silicate (CMAS) deposition: Experiments and first-principles calculation. *Corros. Sci.* **2021**, *182*, 109230. [CrossRef]
24. Fang, H.; Wang, W.; Deng, S.; Yang, T.; Zhu, H.; Huang, J.; Ye, D.; Guo, X. Interaction between Yb_2O_3-Y_2O_3 co-stabilized ZrO_2 ceramic powder and molten silicate deposition, and its implication on thermal barrier coating application. *Mater. Charact.* **2021**, *180*, 111418. [CrossRef]
25. Omata, T.; Kishimoto, H.; Otsuka-Yao-Matsuo, S.; Ohtori, N.; Umesaki, N. Vibrational spectroscopic and X-ray diffraction studies of cerium zirconium oxides with Ce/Zr composition ratio = 1 prepared by reduction and successive oxidation of t'-$(Ce_{0.5}Zr_{0.5})O_2$ phase. *J. Solid State Chem.* **1999**, *147*, 573–583. [CrossRef]
26. Datta, P.; Rihko-Struckmann, L.K.; Sundmacher, K. Quantification of produced hydrogen in a cyclic water gas shift process with Mo stabilized iron oxide. *Fuel Process. Technol.* **2014**, *128*, 36–42. [CrossRef]

27. Ingraci Neto, R.R.; Kardoulaki, E.; Valdez, J.A. The influence of the processing parameters on the reactive flash sintering of ZrO_2-CeO_2. *J. Am. Ceram. Soc.* **2022**, *105*, 3937–3948. [CrossRef]
28. Kurapova, O.Y.; Glukharev, A.G.; Glumov, O.V.; Konakov, V.G. The effect of the sintering parameters on the structure and oxygen ion conductivity of Y_2O_3–ZrO_2–CeO_2 ceramics. *Open Ceram.* **2021**, *5*, 100086. [CrossRef]
29. Wang, Q.; Du, F.; Hou, Y.; Zhang, Y.; Cui, M.; Zhang, Y. Preparation of a CeO_2–ZrO_2 based nano-composite with enhanced thermal stability by a novel chelating precipitation method. *Ceram. Int.* **2021**, *47*, 33057–33063. [CrossRef]
30. Wu, K.; Liu, G.; Yu, P.; Ye, C.; Shi, J.; Shen, Y. Prediction of hardening effect by irradiation-induced vacancy clusters with dislocation dynamics. *Int. J. Plast.* **2022**, *149*, 103160. [CrossRef]
31. Liu, K.; Long, X.; Li, B.; Xiao, X.; Jiang, C. A hardening model considering grain size effect for ion-irradiated polycrystals under nanoindentation. *Nucl. Eng. Technol.* **2021**, *53*, 2960–2967. [CrossRef]
32. Wu, R.; Zaiser, M. Thermodynamic considerations on a class of dislocation-based constitutive models. *J. Mech. Phys. Solids* **2022**, *159*, 104735. [CrossRef]
33. Periyasamy, K.; Aswathy, V.T.; Kumar, V.A.; Manikandan, M.; Shukla, R.; Tyagi, A.K.; Raja, T. An efficient robust fluorite $CeZrO_{4-\delta}$ oxide catalyst for the eco-benign synthesis of styrene. *RSC Adv.* **2015**, *5*, 3619–3626. [CrossRef]
34. Monge, M.A.; Popov, A.I.; Ballesteros, C.; González, R.; Chen, Y.; Kotomin, E.A. Formation of anion-vacancy clusters and nanocavities in thermochemically reduced MgO single crystals. *Phys. Rev. B* **2000**, *62*, 9299. [CrossRef]
35. Lushchik, A.; Dolgov, S.; Feldbach, E.; Pareja, R.; Popov, A.I.; Shablonin, E.; Seeman, V. Creation and thermal annealing of structural defects in neutron-irradiated $MgAl_2O_4$ single crystals. *Nucl. Instrum. Methods Phys. Res. Sect. B Beam Interact. Mater. At.* **2018**, *435*, 31–37. [CrossRef]
36. Pankratov, V.; Popov, A.I.; Chernov, S.A.; Zharkouskaya, A.; Feldmann, C. Mechanism for energy transfer processes between Ce^{3+} and Tb^{3+} in $LaPO_4$: Ce, Tb nanocrystals by time-resolved luminescence spectroscopy. *Phys. Status Solidi B* **2010**, *247*, 2252–2257. [CrossRef]
37. Averback, R.S.; Ehrhart, P.; Popov, A.I.; Sambeek, A.V. Defects in ion implanted and electron irradiated MgO and Al_2O_3. *Radiat. Eff. Defects Solids* **1995**, *136*, 169–173. [CrossRef]
38. Szenes, G.; Pászti, F.; Péter, Á.; Popov, A.I. Tracks induced in TeO_2 by heavy ions at low velocities. *Nucl. Instrum. Methods Phys. Res. Sect. B Beam Interact. Mater. At.* **2000**, *166*, 949–953. [CrossRef]